Front. Mech. Eng. China 2010, 5(2): 226–232
DOI 10.1007/s11465-010-0012-2

RESEARCH ARTICLE

Yiliang ZHANG, Ruibin GOU, Jimin LI, Gongtian SHEN

Characteristics of metal magnetic memory signals of different steels under static tension

Abstract To study the characteristics of metal magnetic memory (MMM) signals of different steels during tensile test, static tension tests were applied to 30 pieces of Q235 and 16MnR base metal and welded specimens. During the various deformation periods, MMM signals are tested, and micrometallographic is observed. Furthermore, the derivative of magnetic intensity (dH_p/dx) is analyzed by mathematical and statistical methods to study the macro and micro corresponding relationships and difference among magnetic signals. Results show that despite the different magnetic intensity (H_p) curves of different materials, their dH_p/dx patterns in the yielding and necking stages are the same; welded specimens have the similar magnetic signal curves with their base metal, and the welded structure does not interfere with its H_p distribution; different materials have their unique zero point ($H_p = 0$) before being fractured, which is independent of the fracture location; there is a direct relationship between the intragranular slip and the changes of magnetic signals, which indicates the uneven plastic deformation.

Keywords metal magnetic memory (MMM), magnetic intensity (H_p), static tension, weld

1 Introduction

Metal magnetic memory testing (MMMT) [1] is a new non-destructive testing (NDT) method that integrates NDT, fracture mechanics, and metallography. Based on the changing magnetic signals on the metal surface with different working loads or stresses, it can effectively detect the stress concentration regions without an external magnetizing field. Therefore, it can be used to diagnose premature defects for ferromagnetic materials and has become a unique practical method to diagnose premature defects of metal structures [2–4].

Researchers have done a great deal of experiments and practical engineering test since MMMT was brought forward, and enabled this technique to be widely used in engineering field [5–7]. Up to now, stress concentration areas are usually determined by the zero points of the MMM curves where H_p is zero and by dH_p/dx breaking. Crack initiation could induce a sudden magnetic leakage in the regions of stress concentrations [8–11]. The immediate demand in engineering is to obtain the stress concentration distribution and the maximum stress according to the measured external magnetic field. Furthermore, potential hazards are still hard to locate before cracking. Therefore, it is difficult to quantitatively analyze the magnetic signals [12,13]. There is now just a tentative study of the relationship between the MMM signals and the material microstructure, and the microcosmic mechanism of MMM signals [14,15]. Researches have found that characteristics of different materials are various. To strictly lay down decision criteria of project structure defects by the MMM method, it is quite necessary to correctly understand the characteristics of MMM signals for various materials (e.g., low carbon steel and low carbon alloy steel) in different stages of deformation.

Widely used for special equipment, research subjects in this paper are 16MnR and Q235 steels. The variations of their magnetic signals during the process of static tension were studied, and microstructure was observed in each stage of deformation. In addition, it comparatively analyzes the magnetic signals' change rules of welded specimens and their base metal, and the magnetic signals' change rules of different materials, and then their differences and relationships for a quantitative analysis of their magnetic signals are summarized both at macro and micro levels. This paper presents foundational datum for further proof of MMMT feasibility in engineering application.

Received October 25, 2009; accepted December 28, 2009

Yiliang ZHANG (✉), Ruibin GOU, Jimin LI, Gongtian SHEN
College of Mechanical Engineering and Applied Electronics Technology, Beijing University of Technology, Beijing 100022, China
E-mail: zhangyil@bjut.edu.cn

2 Test

2.1 Test materials

This paper takes a total number of 30 specimens of 16MnR and Q235 welded and base metal specimens as examine subjects, among which Q235 and 16MnR base metal parts are eight pieces, and their welded specimens are seven pieces, respectively. The chemical composition and mechanical property of the mentioned materials above are listed in Table 1.

Table 1 Chemical composition and mechanical property of materials

material	chemical composition					mechanical property		
	C	Si	Mn	P	S	E /GPa	Rm /MPa	ReL /MPa
16MnR base metal	0.19	0.50	1.51	0.012	0.003	207.6	549.9	398.0
16MnR welded specimens	0.12	0.37	1.42	0.016	0.016	206	560.9	397.2
Q235 base metal	0.16	0.19	0.54	0.021	0.030	193.3	426.9	278.2
Q235 welded specimens	0.16	0.19	0.54	0.021	0.030	200.5	476.2	368.8

2.2 Specimen dimension

The shape design of specimen conforms to national standard which is 7 mm thick, and the other dimensions are shown in Fig. 1. All specimens were annealed at 600°C before testing.

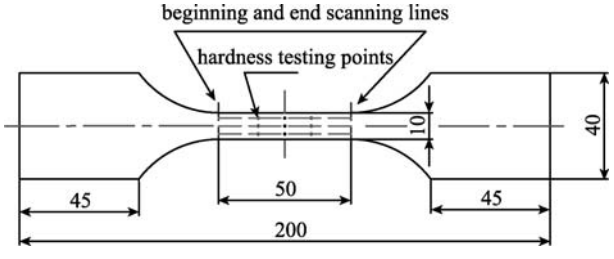

Fig. 1 Chart of specimen dimension

2.3 Equipments

The test devices include the RAS-250 tensile testing machine made in Germany, TSC-1M-4 produced in Russia, VHX-500 digital microscope, and HMV-IT micro-hardness instrument.

2.4 Test methods

1) To study the effect on the magnetic signals due to different test planes, two planes (the horizontal and vertical planes) are detected separately.

2) All specimen planes were labeled as *A* and *B*, and per plane has three checking lines 1, 2, and 3. Among them, line 2 is the center line; the distance between lines 1 and 2 is 3 mm, the distance between line 1 and the nearer edge is 2 mm, and lines 1 and 3 are symmetrical with line 2 as their axis, as is shown in Fig. 2.

3) External magnetic-field interference must be avoided when magnetic signals are tested. Therefore, checking place and scanning path must be the same for each measuring.

4) To further testify the relationship between characteristics of magnetic signals of various materials, microscopic metallographic were observed every time when MMM signals were measured, followed by a quantitative comparative analysis of the microstructure. To have the same point each time, nine hardness test points were marked on the three lines, as shown in Fig. 2.

5) The specimens were tested for the MMM signals in each stage of the deformation, such as elasticity, yield, aggrandizement, and necking stages. Figure 3 shows the tensile curves of the four kinds of specimens, and each Arabic numeral labeled in the charts means that a test has been done at this stress level.

6) Because of the diversity among magnetic signal curves of one specimen in different stages of deformation, linear fitting for magnetic signal curves is required; furthermore, dH_p/dx and its average, variance and standard deviation are worked out to better describe and analyze the change characteristic of magnetic signals during various periods of static tension.

3 Results

Magnetic signal curves of every stage were put together into one graph for better observance and data analyses.

3.1 Magnetic signal results of Q235 and 16MnR base metal specimens

Test results show that two planes (*A* and *B*) have almost the same magnetic signals at the same checking plane, and the magnetic signals of the three testing lines on the same plane (*A* or *B*) are almost identical. Therefore, the magnetic signals of line 2 on plane *B* were taken as examples of Q235 and 16MnR base metal specimens, as shown in Fig. 4.

Figure 4 shows that the magnetic signal curves of the two types of steels are quite approximate beelines with different slopes before necking, and the curves become obviously flexural on the location where micro-cracks occur. Besides, the curves change from skew line to s-shaped after fracturing. To accurately reflect the characteristics of magnetic signals, linear fitting for magnetic signal curves is required; furthermore, dH_p/dx and its average, variance, and standard deviation are worked out. According to statistical error law,the dH_p/dx statistical result is shown in Fig. 5.

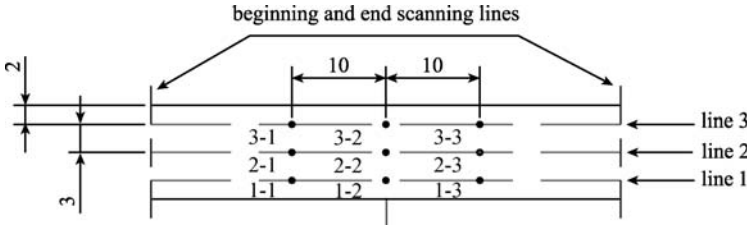

Fig. 2 Scanning lines of MMM and hardness testing points

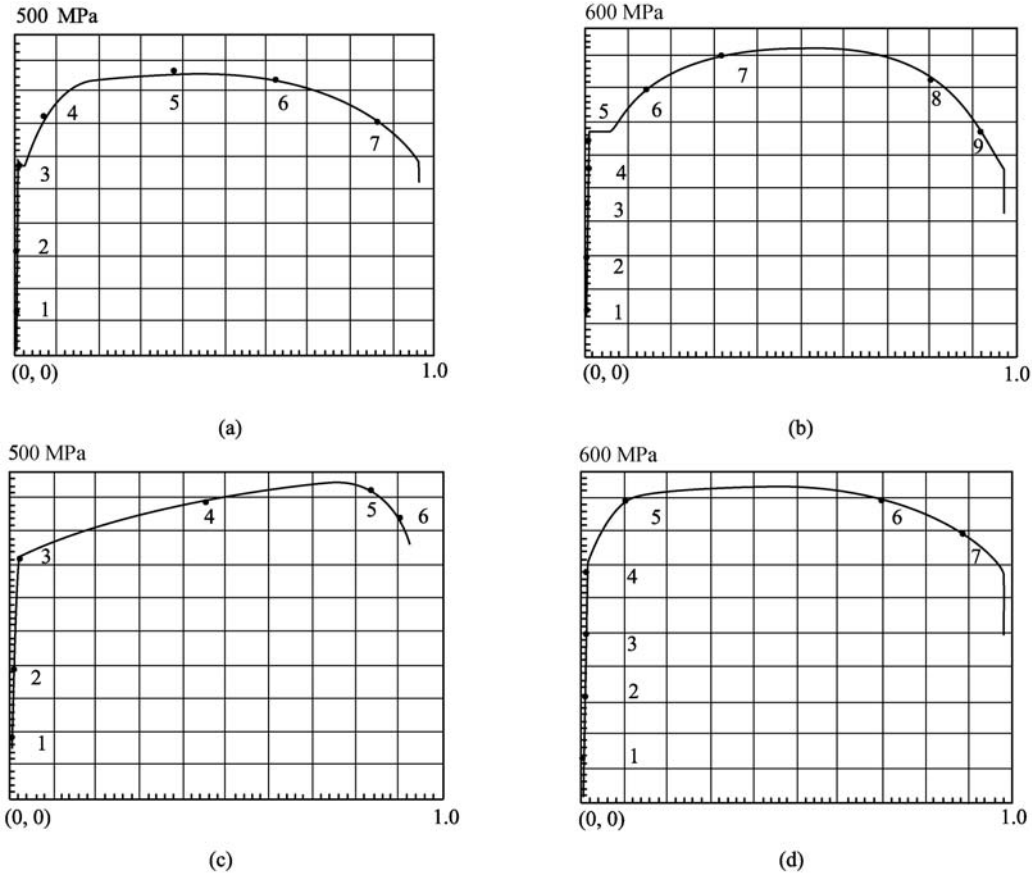

Fig. 3 Tensile curves and test points in each stage. (a) Q235 base metal specimens; (b) 16MnR base metal specimens; (c) Q235 welded specimens; (d) 16MnR welded specimens

3.2 Magnetic signal results of Q235 and 16MnR welded specimens

Because magnetic signals of the four test planes (*A* and *B* horizontal planes, *A* and *B* vertical planes) and the three test lines on the same plane (*A* or *B*) were almost identical, the magnetic signal curves of line 1 in plane A of Q235 and 16MnR welded specimens were taken as an example. Meanwhile, linear fitting was made for the curves in various periods, and the results are shown in Fig. 6.

3.3 Microstructure testing results of Q235 base metal specimens

To have a micro verification of the macroscopic quantity of magnetic signals, magnetic signals were scanned seven times in different stages of the static tension test. Microscopic metallographic structures of the nine hardness test points (as shown in Fig. 7) were observed in stages of before tension, elasticity, yielding, aggrandizement, and necking. The results are shown in Fig. 8.

Figure 8 shows that grain shapes do not change in the first three stages, and they began to change in the stage of aggrandizement. All grains are markedly lathlike, and a great deal of intragranular slip is produced in the necking period.

To obtain the quantitative plastic rules of deformation, diagonal distance of the nine points mentioned above was measured, and corresponding strains were figured out. Tensile direction is defined as axial direction and named *A*,

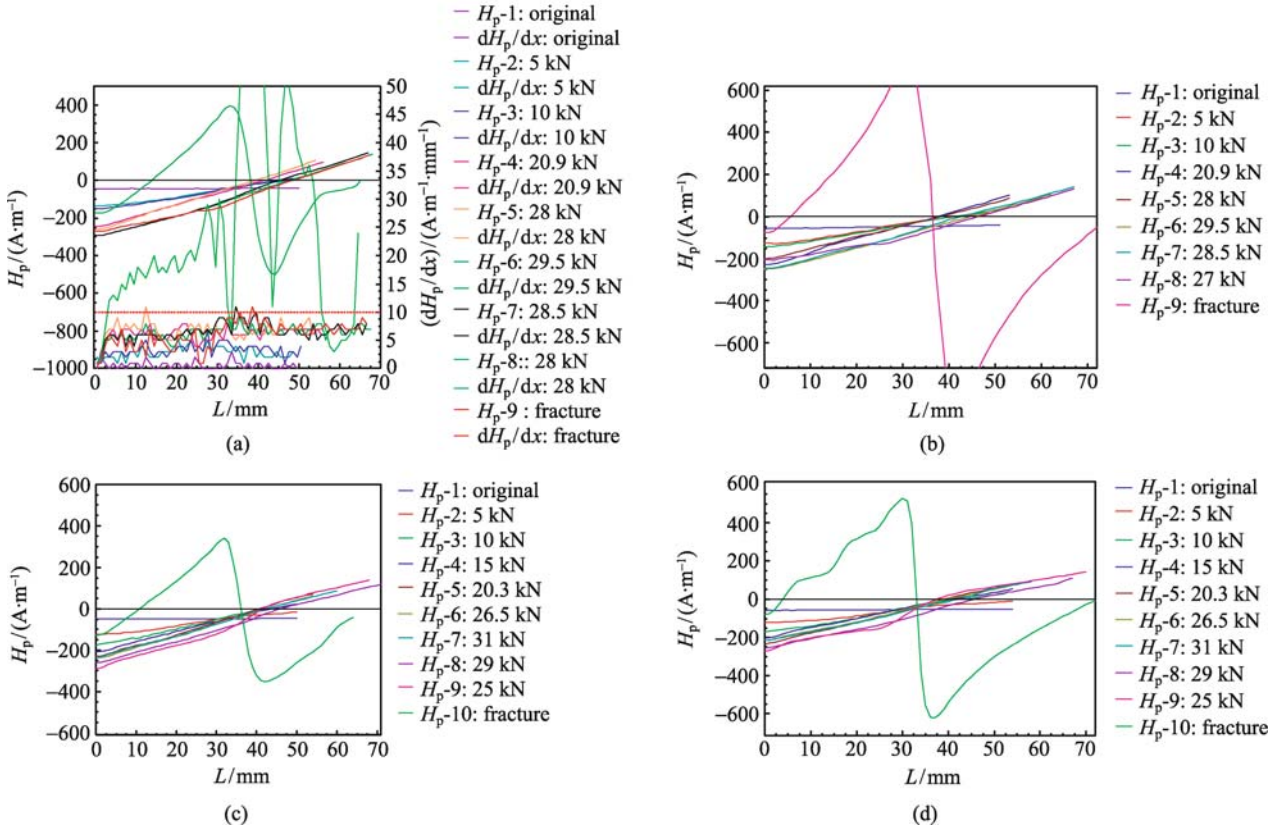

Fig. 4 Typical magnetic signal curves of Q235 and 16MnR base metal specimens. (a) Magnetic signal curve of horizontal plane *B* of Q235 base metal specimens; (b) magnetic signal curve of vertical plane *B* of Q235 base metal specimens; (c) magnetic signal curve of horizontal plane *B* of 16MnR base metal specimens; (d) magnetic signal curve of vertical plane *B* of 16MnR base metal specimens

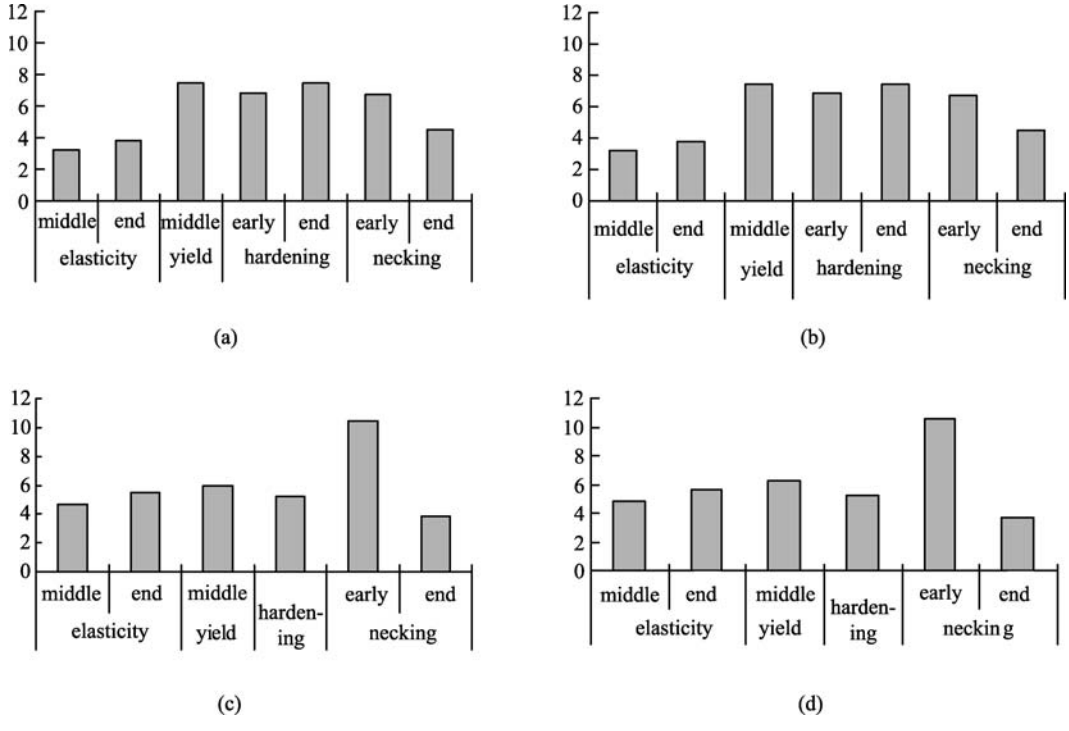

Fig. 5 dH_p/dx change histogram of Q235 and 16MnR base metal specimens. (a) Slope change histogram of Q235 base metal specimens in horizontal plane *B*; (b) slope change histogram of Q235 base metal specimens in vertical plane *B*; (c) slope change histogram of 16MnR base metal specimens in level plane *B*; (d) slope change histogram of 16MnR base metal specimens in vertical plane *B*

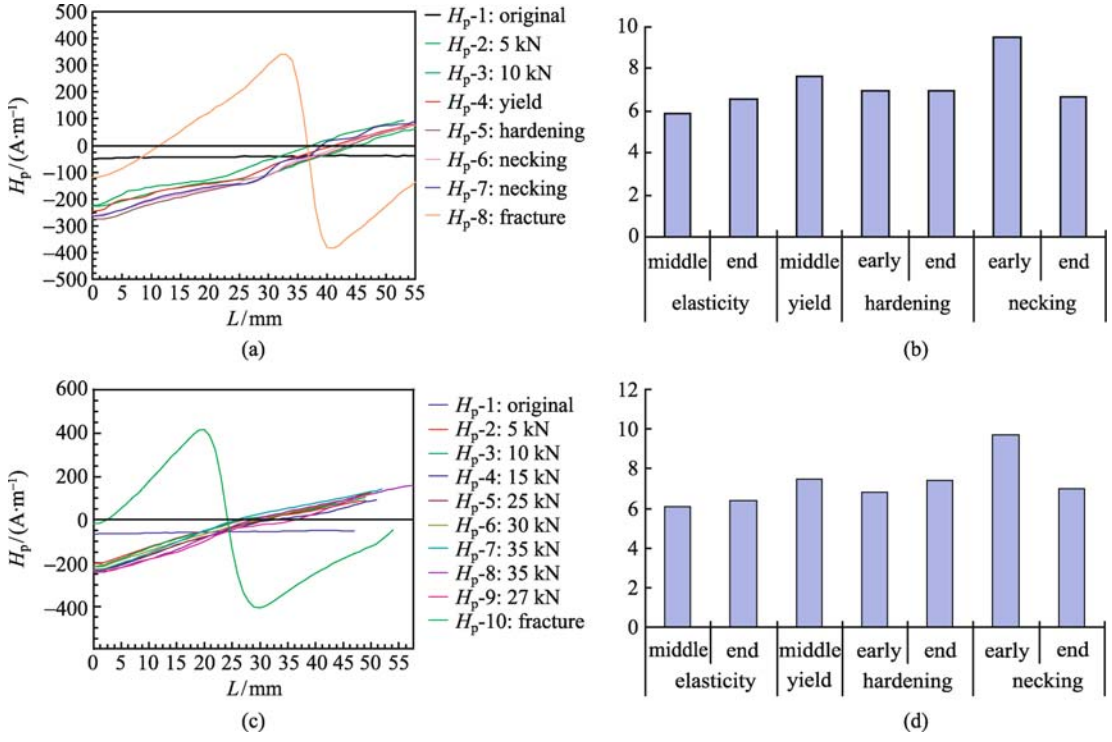

Fig. 6 Curves of magnetic signals and dH_p/dx histogram of Q235 and 16MnR welded specimens. (a) Magnetic signal curves of Q235 welded specimens in horizontal plane A; (b) slope changes histogram of Q235 welded specimens; (c) magnetic signal curves of 16MnR welded specimens in horizontal plane A; (d) slope changes histogram of 16MnR welded specimens

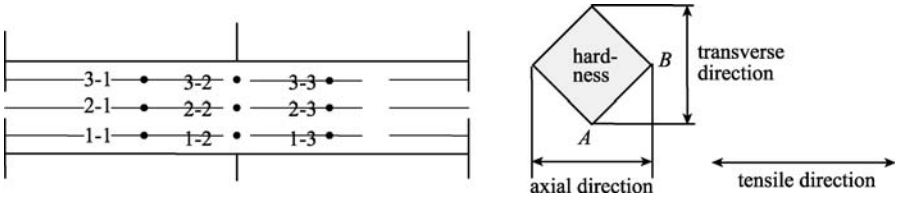

Fig. 7 Schematic diagram of microhardness observation points

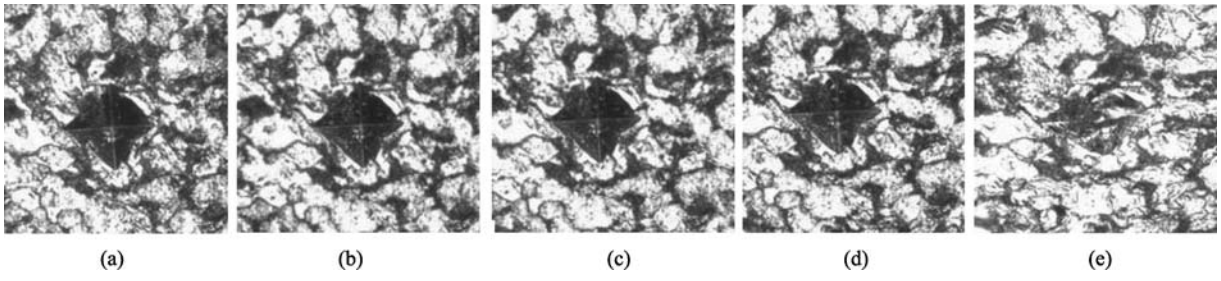

Fig. 8 Microscopic metallographic structures of the hardness test points. (a) Original; (b) elasticity; (c) yielding; (d) aggrandizement; (e) necking

and the vertical direction is named B, as shown in Fig. 7. Because the results of the nine points are nearly the same, this paper takes 3-1 and 1-3 as examples, and the results are shown in Fig. 9.

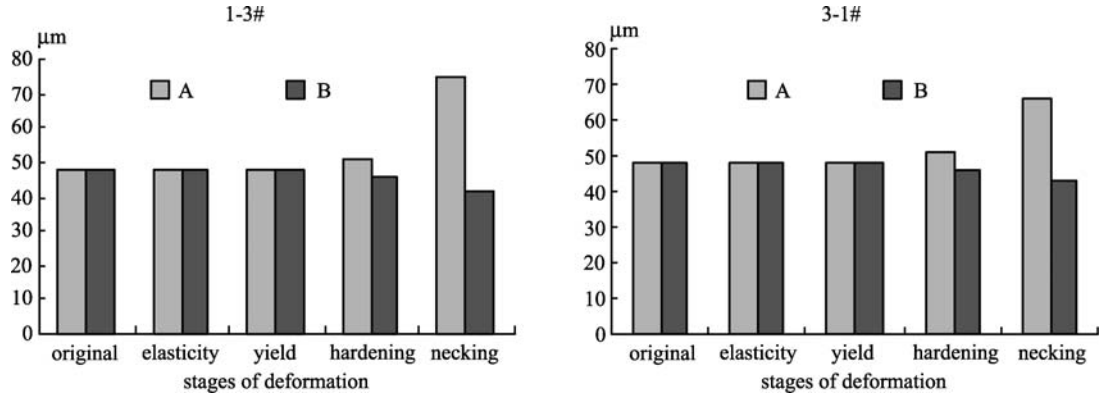

Fig. 9 Diagonal distance change histogram of Q235 base metal specimens' hardness test points in different tensile periods

4 Discussion and analysis

4.1 MMM signal analysis and discussion of Q235 and 16MnR base metal specimens

From Figs. 4 and 5, results can be concluded as follows:

1) MMM signal curves are horizontal lines, and H_p is nearly equal to terrestrial magnetic field intensity before loading; however, the curves become inclined straight lines from horizontal lines after loading.

2) MMM signals reveal the inhomogeneity of plastic deformation. In the yield stage, grain shape does not change, and H_p is evenly distributed. Grain shape changes obviously, and H_p becomes a visible uneven distribution in the necking period.

3) With the increasing deformation, H_p curves keep the characteristics of linearity, and dH_p/dx are basically identical; dH_p/dx of one scanning line apparently changes only when necking appears, and magnetic signals change from inclined straight lines into curves. Furthermore, the location where H_p has an abrupt change is correspondent to the region of the fracture.

4) The two materials' H_p is slightly different. H_p initial position of Q235 is from -300 to -250 A/m; that of 16MnR ranges from -250 to -180 A/m.

5) H_p slopes (dH_p/dx) of the two materials are different. In the initial segment, the slope of 16MnR is higher than that of Q235. When yielded, slopes of 16MnR increase by about 20%, whereas those of Q235 increase by about 96%. Q235 is also higher than 16MnR in the stage of aggrandizement.

6) The location where H_p is equal to zero has nothing to do with the final cracked position, and a great many studies show that MMM curves have a unique zero point before specimen is ruptured; however, it is not the location where the part became fractured. Rupture is just related to dH_p/dx.

7) MMM signals alter sharply when the work-piece was fractured. Furthermore, H_p is equal to zero on the cracked position.

4.2 MMM signal analysis and discussion of Q235 and 16MnR welded specimens

From Fig. 6, results are concluded as follows:

1) Change rules of MMM signals of welded parts are the same as those of base metal specimens, as shown in 1), 2) and 3) of part 4.1.

2) The H_p initial position of the two materials is different. The initial position of Q235 welded part is from -275 to -200 A/m; that of 16MnR ranges from -225 to -200 A/m.

3) dH_p/dx of the two materials are different. In the initial segment, the slope of 16MnR is higher than that of Q235, and dH_p/dx increases when yielded; however, the 16MnR slope is higher in the stage of aggrandizement.

4.3 MMM signal analysis and discussion of welded and base metal specimens

Figure 3 shows that all base metals have a visible yield, and 16MnR is more obvious; however, welded specimens do not. For the same material, magnetic signal characters of welded specimens are the same as those of the base metal parts from 4.1 and 4.2.

4.4 Analysis and discussion of microstructure testing results

Figure 9 shows that grain shape does not change in the former three stages, so do the diagonal distance of hardness test points and microscopic metallographic structures. The grain shape begins to change in the stage of aggrandizement. During the necking period, all grains are markedly lathlike, and intragranular slip is produced. Furthermore, diagonal distance changes markedly. For example, axial strain is about 56%, and transverse strain is about -13%.

The uneven deformation of the measured points further proves the randomness of plastic deformation.

4.5 Analysis and discussion of relationship between MMM signals and microstructure

Compared with Figs. 4(a), 5(a), and 9, dH_p/dx does not change in small deformation during the period of elasticity, so does the grain dimension. dH_p/dx increases greatly at the early stage of yielding. During this stage, uneven plastic deformation is produced, and intragranular slip occurs; however, the grain shape does not change. In the period of aggrandizement, dH_p/dx decreases slightly; however, the grain shape has changed. During the stage of necking, dH_p/dx changes markedly, and the magnetic signal graphs change from the inclined straight line into "S" curves. Moreover, a great deal of intragranular slip is produced, biggish deformation of grains appeared and grains are stripped.

Therefore, intragranular slip is directly related to the changes of magnetic signals.

5 Conclusions

1) H_p change rules of different materials are different.

2) For the same material, magnetic signals of welded specimens are the same as their base metal parts; the welded structure has nothing to do with the distribution rule of H_p.

3) Different materials have their unique zero point ($H_p = 0$) before specimen is fractured; however, the zero point is independent of the fracture location; rupture is just related to dH_p/dx.

4) There is a direct relationship between the intragranular slip and the changes of magnetic signals, which reveals the uneven plastic deformation.

References

1. Dubov A. Diagnostics of metal and equipment by means of metal magnetic memory. In: Proceedings of 7th Conference on NDT and International Research Symposium, Shantou. 1999, 181–187
2. Dubov A. The method of metal magnetic memory— The new trend in engineering diagnostics. Welding in the World, 2005, 49(3): 314–319
3. Zhang Y L, Yang S, Xu X. Application of metal magnetic memory test in failure analysis and safety evaluation of vessels. Frontiers of Mechanical Engineering of China, 2009, 4(1): 40–48
4. Ren J L. Metal magnetic memory testing technique. NDT, 2001, 23 (4): 154–156 (in Chinese)
5. Zhang Y L, Li J M, Shen G T. Analysis about magnetic memory signal and residual stress of 1000 m^3 oil tank. Journal of Beijing University of Technology, 2008, 34(supp): 83–88 (in Chinese)
6. Dubov A. Quality assurance of welded joints in power, chemical and gas pipeline engineering by the method of metal magnetic memory. Welding in the World, 2008, 52: 709–714
7. Li L M, Wang X F, Huang S L. The relationship between metal magnetic memory and geomagnetic field. NDT, 2003, 25(8): 387–390 (in Chinese)
8. Xing H Y, Xu M Q, Zhang J Z. Early damage stress state MMM testing. American Society of Mechanical Engineers, Nondestructive Evaluation Engineering Division (Publication) NDE, 2005, 26: 95–98
9. Yin D W, Xu B S, Dong S Y, Dong L H, Feng C. Chang of magnetic memory signals under different testing environments. ACTA Armamentaria, 2007, 28(3): 319–323 (in Chinese)
10. Zhang J, Zhou K Y. Analysis of the characteristics of the metal magnetic memory signal under different stress states. Journal of Hefei University of Technology, 2007, 30(3): 381–383 (in Chinese)
11. Dong L H, Xu B S, Dong S Y, Song L, Chen Q Z, Shi C L. Discussion of characterizing stress concentration, residual stress and defect by metal magnetic memory testing. Material Engineering, 2009, (8): 19–23 (in Chinese)
12. Liu C K, Tao C H, Chen X, Zhang B, Dong, S Y. Research on quantitative assessment of fatigue damage by metal magnetic memory methods. Material Engineering, 2009, (8): 33–37 (in Chinese)
13. Dong L H, Xu B S, Dong S Y, Chen Q Z, Wang D, Yin D W. The effect of axial tensile load on magnetic memory signals from the surface of medium carbon steel. Chinese Journal of Material Research, 2006, 20(4): 440–444 (in Chinese)
14. Zhou J H, Lei Y Z. The theoretical discussion on magnetic memory phenomenon about positive magnetostriction ferromagnetism materials. Journal of Zhengzhou University, 2003, 24(3): 101–105 (in Chinese)
15. Ren S K, Li X L, Ren J L, Xiao Q Y. Studies on physical mechanism of metal magnetic memory testing technique. Journal of Nanchang Hangkong University, 2008, 22(2): 11–17 (in Chinese)